

# The Discrepancy Between $\tau$ and $e^+e^-$ Spectral Functions Revisited and the Consequences for the Muon Magnetic Anomaly

M. Davier,<sup>3</sup> A. Hoecker,<sup>2</sup> G. López Castro,<sup>4</sup> B. Malaescu,<sup>3</sup> X.H. Mo,<sup>1</sup>  
G. Toledo Sánchez,<sup>5</sup> P. Wang,<sup>1</sup> C.Z. Yuan,<sup>1</sup> and Z. Zhang<sup>3</sup>

<sup>1</sup>*Institute of High Energy Physics, Chinese Academy of Sciences, Beijing*

<sup>2</sup>*CERN, CH-1211, Geneva 23, Switzerland*

<sup>3</sup>*Laboratoire de l'Accélérateur Linéaire, IN2P3/CNRS, Université Paris-Sud 11, Orsay*

<sup>4</sup>*Departamento de Física, Cinvestav, Apartado Postal 14-740, 07000 México D.F., México*

<sup>5</sup>*Instituto de Física, UNAM, A.P. 20-364, 01000 México D.F., México*

(Dated: October 22, 2018)

We revisit the procedure for comparing the  $\pi\pi$  spectral function measured in  $\tau$  decays to that obtained in  $e^+e^-$  annihilation. We re-examine the isospin-breaking corrections using new experimental and theoretical input, and find improved agreement between the  $\tau^- \rightarrow \pi^- \pi^0 \nu_\tau$  branching fraction measurement and its prediction using the isospin-breaking-corrected  $e^+e^- \rightarrow \pi^+\pi^-$  spectral function, though not resolving all discrepancies. We recompute the lowest order hadronic contributions to the muon  $g-2$  using  $e^+e^-$  and  $\tau$  data with the new corrections, and find a reduced difference between the two evaluations. The new tau-based estimate of the muon magnetic anomaly is found to be 1.9 standard deviations lower than the direct measurement.

## I. INTRODUCTION

Spectral functions determined from the cross sections of  $e^+e^-$  annihilation to hadrons are fundamental quantities describing the production of hadrons from the strong interaction vacuum. They are especially useful at low energy where perturbative QCD fails to describe the data. Spectral functions play a crucial role in calculations of hadronic vacuum polarisation (VP) contributions to observables such as the effective electromagnetic coupling at the  $Z^0$  mass, and the muon anomalous magnetic moment. The latter quantity requires good knowledge of the low energy spectral function dominated by the  $\pi^+\pi^-$  channel.

During the last decade, measurements of the  $\pi^+\pi^-$  spectral function with percent accuracy became available [1–4], superseding older and less precise data. The former lack of precision data inspired the search for an alternative. It was found [5] in form of accurate  $\tau^- \rightarrow \pi^- \pi^0 \nu_\tau$  spectral functions [6–9], transferred from the charged to the neutral state using isospin symmetry. With the increasing  $e^+e^- \rightarrow \pi^+\pi^-$  experimental precision, which today is on a level with the  $\tau$  data, systematic discrepancies in shape and normalisation of the spectral functions were observed between the two systems [10, 11]. It was found that, when computing the hadronic VP contribution to the muon magnetic anomaly using the  $\tau$  instead of the  $e^+e^-$  data for the  $2\pi$  and  $4\pi$  channels, the observed deviation with the experimental value [12] would reduce from 3.3 times the combined experimental and estimated theoretical error to less than 1 [13].

In this paper, we include recent  $\tau^- \rightarrow \pi^- \pi^0 \nu_\tau$  data from the Belle experiment [14], and revisit all isospin-breaking corrections in this channel taking advantage of more accurate data and new theoretical investigations.

## II. TAU DATA

The  $\tau$ -based  $a_\mu$  evaluation in [10, 11] used the  $\tau$  spectral functions measured by the ALEPH [7], CLEO [8] and OPAL [9] experiments for the dominant hadronic decay mode  $\tau^- \rightarrow \pi^- \pi^0 \nu_\tau$ . We include here a high-statistics measurement of the same decay mode performed by Belle [14]. Rather different experimental conditions are met at the  $Z$  centre-of-mass energy (ALEPH, OPAL) and at the  $\Upsilon(4S)$  resonance (CLEO, Belle). At LEP the  $\tau^+\tau^-$  events can be selected with high efficiency ( $> 90\%$ ) and small non- $\tau$  background ( $< 1\%$ ), thus ensuring little bias in the efficiency determination. The situation is not as favourable at low energy: because the dominant hadronic cross section has a smaller particle multiplicity, it is more likely to pollute the  $\tau$  sample and strong cuts must be applied, resulting in smaller selection efficiency with larger relative uncertainty. On the other hand, the  $\Upsilon(4S)$  machines outperform LEP in statistics for  $\tau$ -pair production: Belle's analysis contains 5.4 million  $\tau^- \rightarrow h^- \pi^0 \nu_\tau$  candidates ( $72.2 \text{ fb}^{-1}$  integrated luminosity), compared to 81 thousand candidates used by ALEPH (including the full LEP statistics accumulated on the  $Z$  pole). Moreover, CLEO and Belle have an advantage for the  $\tau$  final state reconstruction since particles are more separated in space. The LEP detectors have to cope with collimated  $\tau$  decay products and the granularity of the detectors, particularly the calorimeters, plays a crucial role. One can therefore consider ALEPH/OPAL and CLEO/Belle data to be approximately uncorrelated as far as experimental procedures are concerned.<sup>1</sup> These

<sup>1</sup> Experimental correlations are introduced by common systematic errors in the Monte Carlo simulation used. All experiments employ the same tau decay and radiative corrections libraries, which

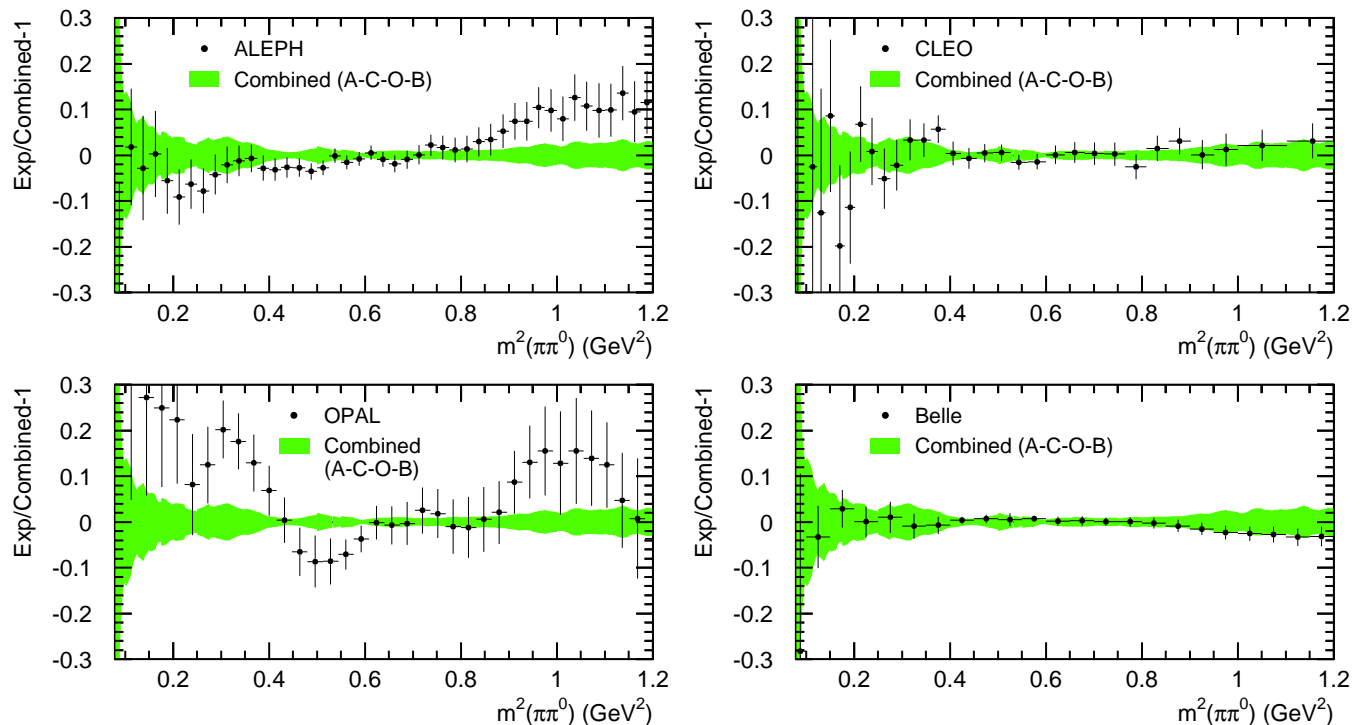


FIG. 1: Relative comparison between the  $\tau^- \rightarrow \pi^- \pi^0 \nu_\tau$  invariant mass-squared measurements from ALEPH, CLEO, OPAL, Belle (data points) and the combined result (shaded band).

four data sets are combined to provide the most precise  $\tau$  spectral function, using the newly developed software package HVPTools [15]. It transforms the original  $\tau$  data and associated statistical and systematic covariance matrices into fine-grained energy bins (1 MeV). In the combination, when the  $\chi^2$  value of a bin-wise average exceeds the number of degrees of freedom ( $n_{\text{dof}}$ ), the error in the averaged bin is rescaled by  $\sqrt{\chi^2/n_{\text{dof}}}$  to account for inconsistencies, which occur because most experiments are dominated by systematic uncertainties. Figure 1 shows the relative comparison of the combined data with those of each experiment.<sup>2</sup>

The branching fraction  $\mathcal{B}_{\pi\pi^0}$  for  $\tau^- \rightarrow \pi^- \pi^0 \nu_\tau$  is obtained from the measured decay channel  $\tau^- \rightarrow h^- \pi^0 \nu_\tau$  ( $\mathcal{B}_{h\pi^0}$ ) by subtracting the non- $\pi$  contribution from the generic charged hadron mode ( $h^-$ ). The average  $\mathcal{B}_{h\pi^0}$  value from these experiments and the two other LEP ex-

periments L3 [17] and DELPHI [18] is  $(25.847 \pm 0.101)\%$ . Subtracting from this the current world average value  $(0.428 \pm 0.015)\%$  for  $\tau^- \rightarrow K^- \pi^0 \nu_\tau$  [19], gives  $\mathcal{B}_{\pi\pi^0} = (25.42 \pm 0.10)\%$ , which is the result used in the following.

### III. ISOSPIN-BREAKING CORRECTIONS

Historically, the conserved vector current (CVC) relation between  $\tau$  and  $e^+e^-$  data was considered even before the discovery of the  $\tau$  lepton [20, 21]. In the limit of isospin invariance, the spectral function of the vector current decay  $\tau \rightarrow X^- \nu_\tau$  is related to the  $e^+e^- \rightarrow X^0$  cross section of the corresponding isovector final state  $X^0$ ,

$$\sigma_{X^0}^{I=1}(s) = \frac{4\pi\alpha^2}{s} v_{1,X^-}(s), \quad (1)$$

where  $s$  is the centre-of-mass energy-squared or equivalently the invariant mass-squared of the  $\tau$  final state  $X$ ,  $\alpha$  is the electromagnetic fine structure constant, and  $v_{1,X^-}$  is the non-strange, isospin-one vector spectral function given by

$$v_{1,X^-}(s) = \frac{m_\tau^2}{6|V_{ud}|^2} \frac{\mathcal{B}_{X^-}}{\mathcal{B}_e} \frac{1}{N_X} \frac{dN_X}{ds} \times \left(1 - \frac{s}{m_\tau^2}\right)^{-2} \left(1 + \frac{2s}{m_\tau^2}\right)^{-1} \frac{R_{\text{IB}}(s)}{S_{\text{EW}}}, \quad (2)$$

are used for the correction of feed-through from non- $h^- \pi^0$  final states, as well as for the determination of the acceptance and efficiency after applying the selection requirements. ALEPH and OPAL use however data-driven spectral functions for the feed-through corrections, so that the resulting correlations should be small. They are hence neglected in the average.

<sup>2</sup> The total systematic uncertainty from Belle is derived from the correlated mass spectra containing revised information with respect to Table V of Ref. [14], which has been provided to us by Belle [16]. They differ mostly at the low mass region below the  $\rho$  mass peak.

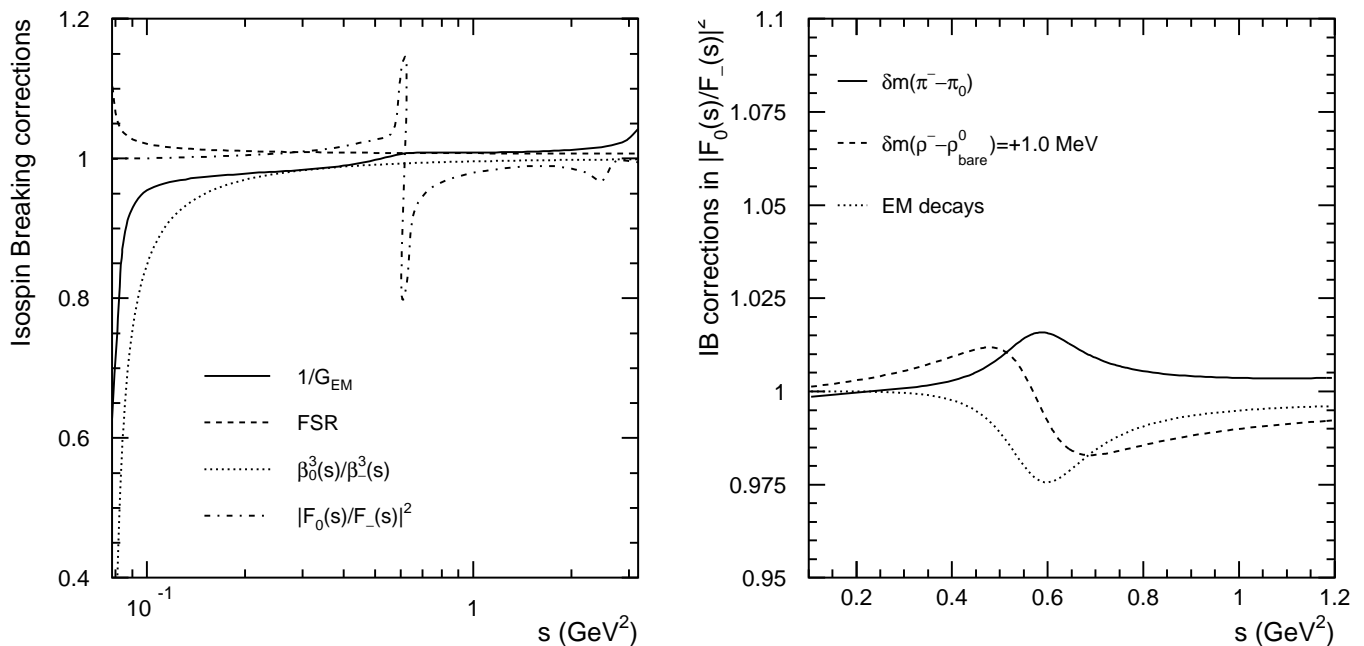


FIG. 2: Left: Isospin-breaking corrections from  $G_{\text{EM}}$ , FSR,  $\beta_0^3(s)/\beta_-^3(s)$  and  $|F_0(s)/F_-(s)|^2$ . Right: Isospin-breaking corrections in the ratio of  $I = 1$  components of the form factors  $|F_0(s)/F_-(s)|^2$  due to the  $\pi$  mass splitting  $\delta m_\pi = m_{\pi^\pm} - m_{\pi^0}$ , the  $\rho$  mass splitting  $\delta m_\rho = m_{\rho^\pm} - m_{\rho_{\text{bare}}^0}$ , and the difference  $\delta\Gamma_\rho$  in the  $\rho$  meson widths.

with

$$R_{\text{IB}}(s) = \frac{\text{FSR}(s)}{G_{\text{EM}}(s)} \frac{\beta_0^3(s)}{\beta_-^3(s)} \left| \frac{F_0(s)}{F_-(s)} \right|^2. \quad (3)$$

In Eq. (2),  $(1/N_X)dN_X/ds$  is the normalised invariant mass spectrum of the hadronic final state, and  $\mathcal{B}_{X^-}$  denotes the branching fraction of  $\tau \rightarrow X^-(\gamma)\nu_\tau$  (throughout this paper, final state photon radiation is implied for  $\tau$  branching fractions). We use for the  $\tau$  mass the value  $m_\tau = (1776.84 \pm 0.17)$  MeV [19], and for the CKM matrix element  $|V_{ud}| = 0.97418 \pm 0.00019$  [22], which assumes CKM unitarity. For the electron branching fraction we use  $\mathcal{B}_e = (17.818 \pm 0.032)\%$ , obtained [23] supposing lepton universality. Short-distance electroweak radiative effects lead to the correction  $S_{\text{EW}} = 1.0235 \pm 0.0003$  [10, 24–26]. All the  $s$ -dependent isospin-breaking (IB) corrections are included in  $R_{\text{IB}}$ , and discussed in the following for the dominant  $\pi\pi$  decay channel.

The first term in Eq. (3) is the ratio  $\text{FSR}(s)/G_{\text{EM}}(s)$ , where  $\text{FSR}(s)$  refers to the final state radiative corrections [27] in the  $\pi^+\pi^-$  channel, and  $G_{\text{EM}}(s)$  denotes the long-distance radiative corrections of order  $\alpha$  to the photon inclusive  $\tau^- \rightarrow \pi^-\pi^0\nu_\tau$  spectrum.  $G_{\text{EM}}(s)$  includes the virtual and real photonic corrections and was calculated originally in [28] in the framework of the Resonance Chiral Theory [29]. In that work the small axial contributions to real photon emission were fixed using the axial anomalous terms [30]. A recalculation of  $G_{\text{EM}}(s)$  was presented in [31], where the real photon corrections were incorporated via a meson dominance model. Since these

corrections diverge in the soft-energy limit, a small mass must be given to the photon as regularisation. Consistency however requires that the real photon corrections are calculated by summing over all three polarisation states of the massive photon [32]. If we include the longitudinal polarisation according to Ref. [32], the model-independent piece of the radiative corrections changes by at most 0.3% close to threshold and rapidly vanishes with increasing  $s$ .

The  $G_{\text{EM}}(s)$  correction used in this analysis is based on Ref. [31]. We do not apply, however, any correction for the contribution from the square of the  $\pi(\omega \rightarrow \pi^0\gamma)$  amplitude, since it is considered as a background by all experiments and hence subtracted from the measured spectral functions. On the other hand, we do keep the interference between bremsstrahlung and  $\omega$  amplitudes. The resulting  $G_{\text{EM}}(s)$  function is shown by the solid curve in the left-hand plot of Fig. 2. The main numerical difference between this correction and that of [28] lies below the  $\rho$  peak. Since the origin of the difference is presently only partly understood, we assign the full effect as systematic uncertainty to the  $G_{\text{EM}}$  correction.

The second correction term in Eq. (3),  $\beta_0^3(s)/\beta_-^3(s)$ , arises from the  $\pi^\pm-\pi^0$  mass splitting and is important only close to the threshold (dotted curve in Fig. 2 (left)).

The third IB correction term involves the ratio of the electromagnetic to weak form factors  $|F_0(s)/F_-(s)|$  and is the most delicate one. Below 1 GeV, the pion form factors are dominated by the  $\rho$  meson resonance, such that IB effects mainly stem from the mass and width

differences between the  $\rho^\pm$  and  $\rho^0$  mesons, and from  $\rho^0$ - $\omega$  mixing. The overall effect of this correction is shown by the dash-dotted curve in Fig. 2 (left).

Let us analyse in more detail the IB effects in the form factors. A direct calculation of the  $2\pi$  production amplitudes in  $e^+e^-$  annihilation and  $\tau$  decays using vector meson dominance leads to

$$F_0(s) = f_{\rho^0}(s) \left[ 1 + \delta_{\rho\omega} \frac{s}{m_\omega^2 - s - im_\omega\Gamma_\omega(s)} \right], \quad (4)$$

$$F_-(s) = f_{\rho^-}(s), \quad (5)$$

where  $\delta_{\rho\omega}$  is a complex  $\rho$ - $\omega$  mixing parameter. Following [7], two phenomenological fits to the  $e^+e^-$  form factor data have been performed using the Gounaris-Sakurai (GS) [33] and Kühn-Santamaria (KS) [34] parametrisations<sup>3</sup>. For the corresponding mixing strengths and phases of the fits we find  $|\delta_{\rho\omega}^{\text{GS}}| = (2.00 \pm 0.06) \times 10^{-3}$ ,  $\arg(\delta_{\rho\omega}^{\text{GS}}) = (11.6 \pm 1.8)^\circ$ , and  $|\delta_{\rho\omega}^{\text{KS}}| = (1.87 \pm 0.06) \times 10^{-3}$ ,  $\arg(\delta_{\rho\omega}^{\text{KS}}) = (13.2 \pm 1.7)^\circ$ , respectively. In both parametrisations, the absorptive parts of the  $\rho$  propagators have an explicit energy-dependence of the form  $-i\sqrt{s}\Gamma_{\rho^{0,-}}(s)$ .

One of the IB effects is associated with the  $\rho$  meson width difference. Within an accuracy of 0.1%, the decay widths of the  $\rho$  mesons below  $\sqrt{s} = 1$  GeV are given by their photon inclusive rates into  $\pi\pi$  modes [38]. A direct calculation of the  $\rho \rightarrow \pi\pi(\gamma)$  and  $\pi\pi\gamma$  decay rates shows that the width difference,  $\delta\Gamma_\rho = \Gamma_{\rho^0} - \Gamma_{\rho^\pm}$ , is given by [38]

$$\delta\Gamma_\rho(s) = \frac{g_{\rho\pi\pi}^2 \sqrt{s}}{48\pi} [\beta_0^3(s)(1 + \delta_0) - \beta_-^3(s)(1 + \delta_-)], \quad (6)$$

where  $g_{\rho\pi\pi}$  is the strong coupling of the isospin-invariant  $\rho\pi\pi$  vertex and  $\delta_{0,-}$  denote radiative corrections for photon-inclusive  $\rho \rightarrow \pi\pi$  decays, which include  $\rho \rightarrow \pi\pi\gamma$ . Contrary to expressions used in previous approaches the  $\rho$  meson decay widths in Eq. (6) are independent of the photon energy cut-off used to separate the  $\rho \rightarrow \pi\pi(\gamma)$  and  $\rho \rightarrow \pi\pi\gamma$  rates. In addition to the IB arising from the  $\pi^\pm - \pi^0$  mass difference, the radiative corrections to  $\rho \rightarrow \pi\pi$  and their corresponding radiative rates produce a splitting in the  $\rho$  meson widths. For instance, at  $\sqrt{s} = m_\rho = 775$  MeV, the width difference of Eq. (6) is  $\delta\Gamma_\rho \approx +0.76$  MeV, compared to the value  $\delta\Gamma_\rho \approx (-0.42 \pm 0.58)$  MeV used in [5]. The difference between the two results is mainly due to the effects from radiative corrections (the  $\delta_{0,-}$  terms in Eq. (6)). Our results can also be compared to the one used in [28],  $\delta\Gamma_\rho =$

$(m_\rho s / 96\pi F_\pi^2) [\beta_0^3(s) - \beta_-^3(s)] + (0.45 \pm 0.45)$  MeV, which at  $\sqrt{s} = 775$  MeV gives  $\delta\Gamma_\rho = (-0.61 \pm 0.45)$  MeV. Note that if electromagnetic effects were ignored ( $\delta_{0,-} = 0$ ) in Eq. (6), we would have  $\delta\Gamma = -1.06$  MeV, which is very similar to the cases considered in [5, 28].

The second input required to assess the IB effects in the form factors is the mass splitting between neutral and charged  $\rho$  mesons. Using the expected difference  $m_{\rho^0} - m_{\rho_{\text{bare}}^0} \approx 3\Gamma(\rho^0 \rightarrow e^+e^-)/(2\alpha) = 1.45$  MeV, between dressed and bare  $\rho^0$  mass [39], together with the experimental value  $m_{\rho^\pm} - m_{\rho^0} = (-0.4 \pm 0.9)$  MeV, obtained by KLOE from a fit to the  $\phi \rightarrow \pi^+\pi^-\pi^0$  Dalitz plot [40], one finds  $\delta m_\rho = m_{\rho^\pm} - m_{\rho_{\text{bare}}^0} = (1.0 \pm 0.9)$  MeV, which we use here instead of the degeneracy assumed in previous analyses [10, 28].

The IB effects in the ratio of  $I = 1$  components of the pion form factors (except for  $\rho$ - $\omega$  mixing) are drawn in the right-hand plot of Fig. 2. It is noticeable that the effects of photonic corrections and of the  $\pi^\pm - \pi^0$  mass difference in the  $\rho$  meson widths largely cancel each other.

Figure 3 shows the relative difference between the  $e^+e^-$  and the isospin-breaking-corrected  $\tau$  spectral functions versus  $s$ . The relative normalisation is consistent within the respective errors and the shape is found in better agreement than before [11], despite a remaining deviation above the  $\rho$ -mass-squared. The discrepancy with the KLOE data, although reduced, persists.

#### IV. UPDATE OF $a_\mu^{\text{had,LO}}[\pi\pi, \tau]$

TABLE I: Contributions to  $a_\mu^{\text{had,LO}}[\pi\pi, \tau]$  ( $\times 10^{-10}$ ) from the isospin-breaking corrections discussed in Sec. III. Corrections shown in two separate columns correspond to the Gounaris-Sakurai (GS) and Kühn-Santamaria (KS) parametrisations, respectively.

Source	$\Delta a_\mu^{\text{had,LO}}[\pi\pi, \tau]$ ( $10^{-10}$ )	
	GS model	KS model
$S_{\text{EW}}$	$-12.21 \pm 0.15$	
$G_{\text{EM}}$	$-1.92 \pm 0.90$	
FSR	$+4.67 \pm 0.47$	
$\rho$ - $\omega$ interference	$+2.80 \pm 0.19$	$+2.80 \pm 0.15$
$m_{\pi^\pm} - m_{\pi^0}$ effect on $\sigma$	$-7.88$	
$m_{\pi^\pm} - m_{\pi^0}$ effect on $\Gamma_\rho$	$+4.09$	$+4.02$
$m_{\rho^\pm} - m_{\rho_{\text{bare}}^0}$	$0.20^{+0.27}_{-0.19}$	$0.11^{+0.19}_{-0.11}$
$\pi\pi\gamma$ , electrom. decays	$-5.91 \pm 0.59$	$-6.39 \pm 0.64$
Total	$-16.07 \pm 1.22$	$-16.70 \pm 1.23$
	$-16.07 \pm 1.85$	

The IB corrections applied to the lowest order hadronic contribution to the muon  $g - 2$  using  $\tau$  data in the dom-

<sup>3</sup> The fits are performed in the full mass range where the  $e^+e^-$  data are available. This differs from those fits performed in Ref. [35] in which the fits were limited to a given single  $e^+e^-$  experiment (with data available only below 1 GeV) with fewer number of free parameters. We do not use the Hidden Local Symmetry effective model [36] and the effective field theory model [37] as these models do not include contributions from the high mass resonances such as  $\rho'$  and therefore can only be valid for the mass range below about 1 GeV.

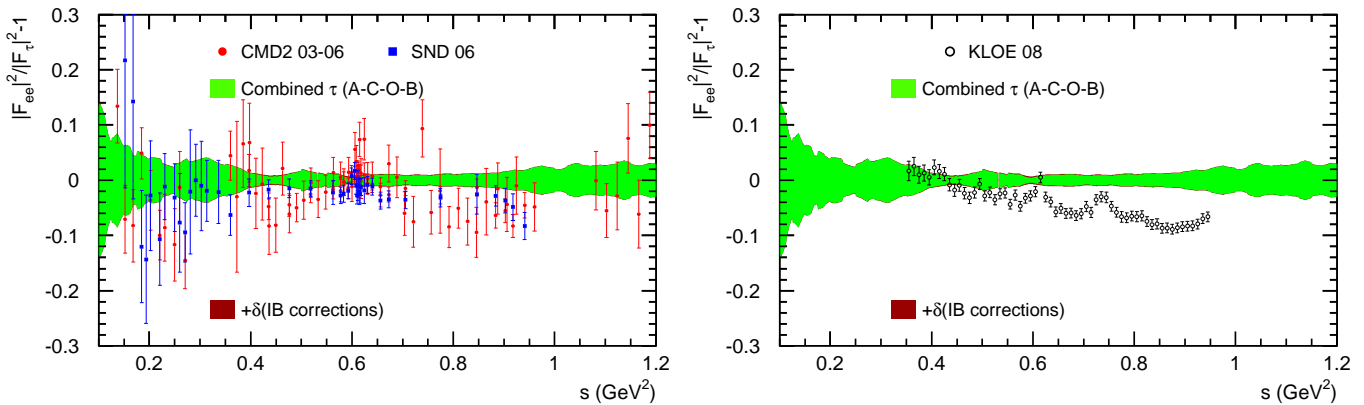


FIG. 3: Relative comparison between  $e^+e^-$  and  $\tau$  spectral functions, expressed in terms of the difference between neutral and charged pion form factors. Isospin-breaking (IB) corrections are applied to  $\tau$  data with its uncertainties, although hardly visible, included in the error band.

TABLE II: The IB-corrected  $a_\mu^{\text{had,LO}}[\pi\pi, \tau]$  ( $\times 10^{-10}$ ) from the measured mass spectrum by ALEPH, CLEO, OPAL and Belle, and the combined spectrum using the corresponding branching fraction values. The results are shown separately in two different energy ranges. The first errors are due to the shapes of the mass spectra, which also include a small contribution of 0.11 from the  $\tau$  mass and  $|V_{ud}|$ . The second errors are due to  $\mathcal{B}_{\pi\pi^0}$  and  $\mathcal{B}_e$ , and the third errors from the isospin-breaking corrections, which are partially anti-correlated between the two energy ranges. The last line gives the world average branching fraction and also the evaluations of the combined spectra (which are not equivalent to the arithmetic averages of the individual evaluations – see text).

Experiment	$a_\mu^{\text{had,LO}}[\pi\pi, \tau]$ ( $10^{-10}$ )		$\mathcal{B}_{\pi\pi^0}$ (%)
	$2m_{\pi^\pm} - 0.36$ GeV	$0.36 - 1.8$ GeV	
ALEPH	$9.46 \pm 0.33_{\text{exp}} \pm 0.05_{\mathcal{B}} \pm 0.07_{\text{IB}}$	$499.19 \pm 5.20_{\text{exp}} \pm 2.70_{\mathcal{B}} \pm 1.87_{\text{IB}}$	$25.49 \pm 0.10_{\text{stat}} \pm 0.09_{\text{syst}}$
CLEO	$9.65 \pm 0.42_{\text{exp}} \pm 0.17_{\mathcal{B}} \pm 0.07_{\text{IB}}$	$504.51 \pm 5.36_{\text{exp}} \pm 8.77_{\mathcal{B}} \pm 1.87_{\text{IB}}$	$25.44 \pm 0.12_{\text{stat}} \pm 0.42_{\text{syst}}$
OPAL	$11.31 \pm 0.76_{\text{exp}} \pm 0.15_{\mathcal{B}} \pm 0.07_{\text{IB}}$	$515.56 \pm 9.98_{\text{exp}} \pm 6.95_{\mathcal{B}} \pm 1.87_{\text{IB}}$	$25.46 \pm 0.17_{\text{stat}} \pm 0.29_{\text{syst}}$
Belle	$9.74 \pm 0.28_{\text{exp}} \pm 0.15_{\mathcal{B}} \pm 0.07_{\text{IB}}$	$503.95 \pm 1.90_{\text{exp}} \pm 7.84_{\mathcal{B}} \pm 1.87_{\text{IB}}$	$25.24 \pm 0.01_{\text{stat}} \pm 0.39_{\text{syst}}$
Combined	$9.76 \pm 0.14_{\text{exp}} \pm 0.04_{\mathcal{B}} \pm 0.07_{\text{IB}}$	$505.46 \pm 1.97_{\text{exp}} \pm 2.19_{\mathcal{B}} \pm 1.87_{\text{IB}}$	$25.42 \pm 0.10$

inant  $\pi\pi$  channel can be evaluated with

$$\Delta^{\text{IB}} a_\mu^{\text{LO, had}}[\pi\pi, \tau] = \frac{\alpha^2 m_\tau^2}{6 |V_{ud}|^2 \pi^2} \frac{\mathcal{B}_{\pi\pi^0}}{\mathcal{B}_e} \int_{4m_\pi^2}^{m_\tau^2} ds \frac{K(s)}{s} \\ \times \frac{dN_X}{N_X ds} \left(1 - \frac{s}{m_\tau^2}\right)^{-2} \left(1 + \frac{2s}{m_\tau^2}\right)^{-1} \left[ \frac{R_{\text{IB}}(s)}{S_{\text{EW}}} - 1 \right],$$

where  $K(s)$  is a QED kernel function [41].

The numerical values for the various corrections are given in Table I for the energy range between the  $2\pi$  mass threshold and 1.8 GeV. The present estimate of the IB effect from long-distance corrections is smaller than the previous one [13, 31], because we now use a  $G_{\text{EM}}(s)$  correction in which the contributions involving the  $\rho\omega\pi$  vertex are explicitly excluded (except for its interference with the QED amplitude). Its uncertainty corresponds to the difference between the correction used in this analysis and that from Ref. [28]. The quoted 10% uncertainty on the FSR and  $\pi\pi\gamma$  electromagnetic corrections is an estimate of the structure-dependent effects (pion form factor) in virtual corrections and of intermediate reso-

nance contributions to real photon emission [38, 42, 43]. The systematic uncertainty assigned to the  $\rho-\omega$  interference contribution accounts for the difference in  $a_\mu^{\text{had,LO}}$  between two phenomenological fits, where the mass and width of the  $\omega$  resonance are either left free to vary or fixed to their world average values.

Some of the corrections in Table I are parametrisation dependent. We choose to take the final corrections from the Gounaris-Sakurai parametrisation and assign the full difference with respect to the KS results<sup>4</sup> as systematic error. The total correction for isospin breaking amounts to  $(-16.07 \pm 1.85) \cdot 10^{-10}$  for  $a_\mu^{\text{had,LO}}[\pi\pi, \tau]$ , where all systematic errors have been added in quadrature except for the GS and KS difference which has been added linearly. This correction is to be compared to the value

<sup>4</sup> We do not confirm the significant IB correction difference of the KS parametrisation on the  $\rho-\omega$  interference with respect to the GS parametrisation observed in Ref. [35].



$(-13.8 \pm 2.4) \cdot 10^{-10}$  obtained previously [10]. Since the FSR correction was previously included, but not counted in the IB corrections, the net change amounts to  $-6.9 \times 10^{-10}$ , dominated by the electromagnetic decay correction.

The corresponding IB-corrected  $a_\mu^{\text{had,LO}}[\pi\pi, \tau]$  in the dominant  $\pi^+\pi^-$  channel below 1.8 GeV is given in Table II for ALEPH, CLEO, OPAL, Belle, and for the combined mass spectrum from these experiments. The evaluation at energy below 0.36 GeV is obtained by fitting an expansion in  $s$  to the corresponding mass spectrum following the method introduced in [10]. The comparison of the fit with the  $\tau$  data at low energy is shown in Fig. 4 (left). Good agreement is observed. Indeed, a direct determination using data gives  $(10.18 \pm 0.98_{\text{exp}}) \times 10^{-10}$  in agreement with the fit-based result of  $(9.76 \pm 0.14_{\text{exp}}) \times 10^{-10}$ , which is more precise because of the constraint  $F(0) = 1$ . The evaluation in the remaining energy region is performed directly from a finely (1 MeV) binned mass spectrum obtained using HVPTools by interpolating the original measurements with second order polynomials (conserving by means of renormalisation the integral in each bin before and after interpolation). The consistent propagation of all errors is ensured by generating large samples of pseudo Monte Carlo experiments. The uncertainty due to the interpolation procedure is estimated from a test with a known model to be at most  $0.2 \times 10^{-10}$ , which is negligible compared to the other systematic uncertainties. It is interesting to compare the first and second errors between the experiments. The first errors are mainly experimental, but also include small contributions from the uncertainties in  $\tau$  mass and  $|V_{ud}|$ . The second errors are due to  $\mathcal{B}_{\pi\pi^0}$ , as measured by each experiment, and – to a lesser extent – to  $\mathcal{B}_e$ , for which a common value has been used everywhere. Belle has the most precise experimental precision on the measurement of the mass spectrum, whereas ALEPH dominates the  $\mathcal{B}_{\pi\pi^0}$  measurement. The result  $a_\mu^{\text{had,LO}}[\pi\pi, \tau] = 515.2 \pm 2.0_{\text{exp}} \pm 2.2_{\mathcal{B}} \pm 1.9_{\text{IB}}$  (if not stated otherwise, this and the following numbers for  $a_\mu$  are given in units of  $10^{-10}$ ) is obtained from the combined  $\pi^-\pi^0$  mass spectrum of ALEPH, CLEO, OPAL and Belle using the world average  $\mathcal{B}_{\pi\pi^0} = (25.42 \pm 0.10)\%$ . This result is consistent with the direct average  $516.1 \pm 1.8_{\text{exp}} \pm 2.2_{\mathcal{B}} \pm 1.9_{\text{IB}}$ , obtained from the four individual  $a_\mu$  calculations. The experimental error from the combined spectrum is slightly less precise as it accounts for the incompatibility between experiments in certain region of the mass spectrum.

The contributions to  $a_\mu^{\text{had,LO}}$  from the  $\pi^+\pi^-2\pi^0$  and  $2\pi^+2\pi^-$  channels below 1.8 GeV are  $21.4 \pm 1.3_{\text{exp}} \pm 0.6_{\text{IB}}$  and  $12.3 \pm 1.0_{\text{exp}} \pm 0.4_{\text{IB}}$ , respectively. This leads to the complete  $\tau$ -based lowest order hadronic contribution

$$\begin{aligned} a_\mu^{\text{had,LO}}[\tau] &= 705.3 \pm 3.9_{\text{exp}} \pm 0.7_{\text{rad}} \pm 0.7_{\text{QCD}} \pm 2.1_{\text{IB}}, \\ &= 705.3 \pm 4.5, \end{aligned} \quad (7)$$

where the second error is due to our treatment of (potentially) missing radiative corrections in old data included in the calculation of the dispersion integral [11], and the

third error stems from the uncertainty in the perturbative evaluation of the inclusive hadronic cross section in the energy ranges 1.8–3.7 GeV and beyond 5 GeV. The central value decreases from previously 710.3, obtained using incomplete isospin corrections [13] and the superseded combined  $\tau$  spectral function from ALEPH, CLEO and OPAL.

We also re-evaluate the lowest order hadronic contribution to the muon  $g - 2$  using  $e^+e^-$  data, updating our most recent preliminary result [13] with published CMD-2 [2] and KLOE [4] data. The results are given in Table III. We have separated the evaluation into four distinct energy ranges. The most recent  $e^+e^-$  data from CMD2, SND and KLOE overlap in the range 0.63–0.958 GeV so that the corresponding  $a_\mu^{\text{had,LO}}[\pi\pi, e^+e^-]$  values can be compared. Agreement is observed between CMD2 and SND, while KLOE lies somewhat lower. To account for this, we consider two combinations of the  $e^+e^-$  data, distinguished by either including or excluding the KLOE data. The combination of the data is performed also using HVPTools [15], to transform the original  $e^+e^-$  bare cross sections and associated statistical and systematic covariance matrices into fine-grained energy bins (1 MeV), taking into account to our best knowledge the correlation within each experiment as well as between the experiments. The evaluation in the low energy range  $2m_{\pi^\pm} - 0.36$  GeV is performed as for the  $\tau$  data by fitting an expansion in  $s$  to the combined  $e^+e^-$  data [10] (right-hand plot of Fig. 4), benefiting from additional space-like precision data [44]. The evaluations in the other three energy ranges are obtained by integrating directly the combined  $e^+e^-$  cross sections (*cf.* Table III).

We find for the difference,  $\delta a_\mu^{\text{had,LO}}[\pi\pi]$ , between the  $\tau$  and  $e^+e^-$ -based evaluations in the dominant  $\pi^+\pi^-$  channel

$$\delta a_\mu^{\text{had,LO}}[\pi\pi] = \begin{cases} 11.7 \pm 3.5_{ee} \pm 3.5_{\tau+\text{IB}}, \\ 10.6 \pm 4.3_{ee} \pm 3.5_{\tau+\text{IB}}, \end{cases} \quad (8)$$

where the upper (lower) value is for KLOE data included (excluded). The discrepancies amount to 2.4 and 1.9 times the overall errors, respectively.

Including the contributions from the other hadronic channels [13], we find for the total  $e^+e^-$ -based lowest order hadronic evaluation

$$a_\mu^{\text{had,LO}}[e^+e^-] = \begin{cases} 689.8 \pm 4.3_{\text{exp+rad}} \pm 0.7_{\text{QCD}}, \\ 690.9 \pm 5.2_{\text{exp+rad}} \pm 0.7_{\text{QCD}}, \end{cases}$$

with total errors of 4.4(5.2) when including (excluding) KLOE. Adding the other contributions [13] including the latest estimate of the light-by-light scattering (LBLS) contribution of  $10.5 \pm 2.6$  [45], we obtain the Standard Model predictions (still in  $10^{-10}$  units)

$$\begin{aligned} a_\mu^{\text{SM}}[\tau] &= 11\,659\,193.2 \pm 4.5 \pm 2.6 \pm 0.2, \\ a_\mu^{\text{SM}}[e^+e^-] &= \begin{cases} 11\,659\,177.7 \pm 4.4 \pm 2.6 \pm 0.2, \\ 11\,659\,178.8 \pm 5.2 \pm 2.6 \pm 0.2, \end{cases} \end{aligned}$$

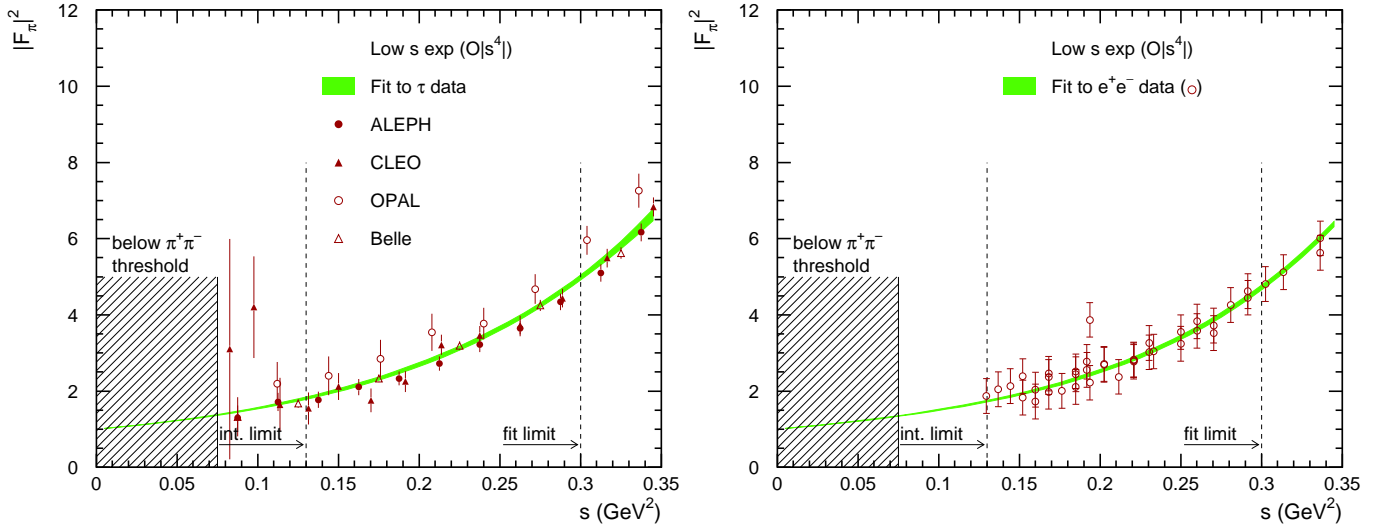


FIG. 4: Fit of the pion form factor from  $4m_\pi^2$  to  $0.3\text{ GeV}^2$  using a third order expansion with the constraints  $F(0) = 1$  and using the measured pion charge radius-squared from space-like data [44]. The result of the fit to the  $\tau$  data (left) and to  $e^+e^-$  data (right) is integrated only up to  $0.13\text{ GeV}^2$ , beyond which we directly integrate over the data points.

TABLE III: Evaluated  $a_\mu^{\text{had,LO}}[\pi\pi, e^+e^-]$  ( $\times 10^{-10}$ ) contribution from the  $e^+e^-$  data, including and excluding KLOE data. The errors correspond to the experimental uncertainties with the statistical and systematical errors added in quadrature (but shown separately for individual experiments).

Energy range (GeV)	Experiment	$a_\mu^{\text{had,LO}}[\pi\pi, e^+e^-]$ ( $10^{-10}$ )	
		Incl. KLOE	Excl. KLOE
$2m_{\pi^\pm} - 0.36$	Combined $e^+e^-$ (fit)	$9.71 \pm 0.12_{\text{exp}}$	
$0.36 - 0.63$	Combined $e^+e^-$	$120.27 \pm 1.67_{\text{exp}}$	$119.63 \pm 1.88_{\text{exp}}$
$0.63 - 0.958$	CMD2 03	$361.82 \pm 2.43_{\text{stat}} \pm 2.10_{\text{sys}}$	
	CMD2 06	$360.17 \pm 1.75_{\text{stat}} \pm 2.83_{\text{sys}}$	
	SND 06	$360.68 \pm 1.38_{\text{stat}} \pm 4.67_{\text{sys}}$	
	KLOE 08	$356.82 \pm 0.39_{\text{stat}} \pm 3.08_{\text{sys}}$	
	Combined $e^+e^-$	$358.51 \pm 2.41_{\text{exp}}$	$360.24 \pm 3.02_{\text{exp}}$
$0.958 - 1.8$	Combined $e^+e^-$	$15.02 \pm 0.36_{\text{exp}}$	$15.02 \pm 0.39_{\text{exp}}$
Total	Combined $e^+e^-$	$503.51 \pm 3.47_{\text{exp}}$	$504.60 \pm 4.33_{\text{exp}}$

where the first errors are due to the lowest order hadronic contributions, the second error includes higher hadronic orders, dominated by the uncertainty in the LBLS contribution, and the third error accounts for the uncertainties in the electromagnetic and weak contributions. The predictions deviate from the experimental average,  $a_\mu^{\text{exp}} = 11\,659\,208.9(5.4)(3.3)$  [46, 47], by  $15.7 \pm 8.2$  ( $\tau$ ),  $31.2 \pm 8.1$  ( $e^+e^-$  with KLOE) and  $30.1 \pm 8.6$  ( $e^+e^-$  without KLOE), respectively.

The lowest order hadronic contribution now reaches an uncertainty that is smaller than the measurement error and comparable in size with the LBLS uncertainty. Further progress in this field thus requires, apart from continuously improved low-energy  $e^+e^-$  cross section mea-

surements, a more accurate muon  $g-2$  measurement and LBLS calculation. A compilation of this and other recent  $a_\mu^{\text{SM}}$  predictions, compared to the experimental value, is shown in Fig. 5.

## V. CVC PREDICTION OF $\mathcal{B}_{\pi\pi 0}$

The CVC relation (1) allows one to predict the branching fraction of a heavy lepton decaying into a  $G$ -parity even hadronic final state,  $X^-$ , via the vector current

$$\mathcal{B}_X^{\text{CVC}} = \frac{3}{2} \frac{\mathcal{B}_e |V_{ud}|^2}{\pi \alpha^2 m_\tau^2} \int_{s_{\text{min}}}^{m_\tau^2} ds s \sigma_{X^0}^I \left(1 - \frac{s}{m_\tau^2}\right)^2 \left(1 + \frac{2s}{m_\tau^2}\right),$$

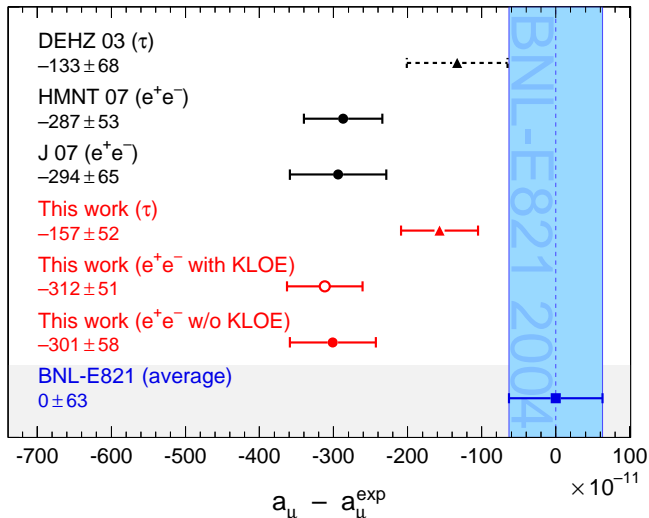


FIG. 5: Compilation of recently published results for  $a_\mu^{\text{SM}}$  (in units of  $10^{-11}$ ), subtracted by the central value of the experimental average [46, 47]. The shaded band indicates the experimental error. The SM predictions are taken from: DEHZ 03 [11], HMNT 07 [48], J 07 [49], and the present  $\tau$ - and  $e^+e^-$ -based predictions using  $\tau$  and  $e^+e^-$  spectral functions.

TABLE IV: Contributions to  $\mathcal{B}_{\pi^-\pi^0}^{\text{CVC}}$  ( $\times 10^{-2}$ ) from the isospin-breaking corrections discussed in Sec. III. For those corrections shown in two separated columns, they correspond to the Gounaris-Sakurai and Kühn-Santamaria parametrisations, respectively.

Source	$\Delta\mathcal{B}_{\pi^-\pi^0}^{\text{CVC}}$ ( $10^{-2}$ )	
	GS model	KS model
$S_{\text{EW}}$	$+0.57 \pm 0.01$	
$G_{\text{EM}}$	$-0.07 \pm 0.17$	
FSR	$-0.19 \pm 0.02$	
$\rho$ - $\omega$ interference	$-0.01 \pm 0.01$	$-0.02 \pm 0.01$
$m_{\pi^\pm} - m_{\pi^0}$ effect on $\sigma$		$+0.19$
$m_{\pi^\pm} - m_{\pi^0}$ effect on $\Gamma_\rho$		$-0.22$
$m_{\rho^\pm} - m_{\rho_{\text{bare}}^0}$	$+0.08 \pm 0.08$	$+0.09 \pm 0.08$
$\pi\pi\gamma$ , electrom. decays	$+0.34 \pm 0.03$	$+0.37 \pm 0.04$
Total	$+0.69 \pm 0.19$	$+0.72 \pm 0.19$
	$+0.69 \pm 0.22$	

with  $s_{\text{min}}$  being the threshold of the invariant mass-squared of the final state  $X^0$  in  $e^+e^-$  annihilation. This relation was tested ever since the discovery of the  $\tau$  lepton. In the best known vector channel, the  $\pi^-\pi^0$  final state, it has attained a precision of better than 1% [13], and a discrepancy between  $\mathcal{B}_{\pi^-\pi^0}^{\text{CVC}}$  and  $\mathcal{B}_{\pi^-\pi^0}$  at a level

of  $4.5\sigma$  was observed.<sup>5</sup> CVC comparisons of  $\tau$  branching fractions are of special interest because they are essentially insensitive to the shape of the  $\tau$  spectral function, hence avoiding experimental difficulties, such as the mass dependence of the  $\pi^0$  detection efficiency and feed-through, and biases from the unfolding of the raw mass distribution from acceptance and resolution effects.

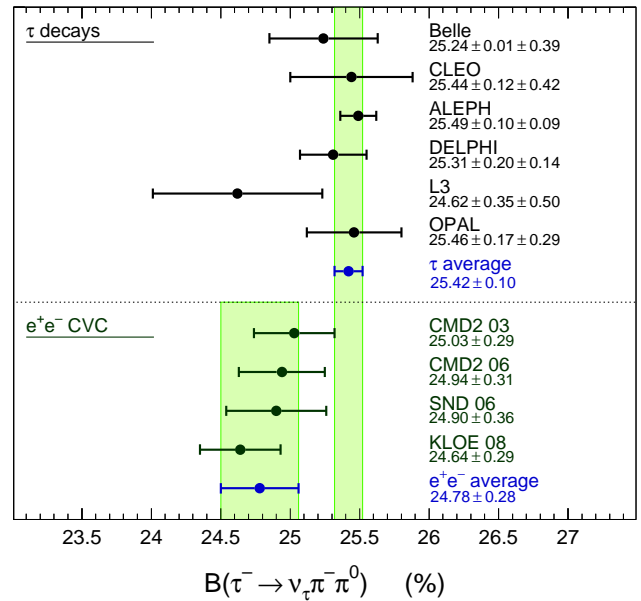


FIG. 6: The measured branching fractions for  $\tau^- \rightarrow \pi^-\pi^0\nu_\tau$  [7–9, 14, 17, 18] compared to the predictions from the  $e^+e^- \rightarrow \pi^+\pi^-$  spectral functions, applying the isospin-breaking corrections discussed in Sec. III. For the  $e^+e^-$  results, we have used only the data from the indicated experiments in  $0.63 - 0.958$  GeV and the combined  $e^+e^-$  data in the remaining energy domains below  $m_\tau$ . The long and short vertical error bands correspond to the  $\tau$  and  $e^+e^-$  averages of  $(25.42 \pm 0.10)\%$  and  $(24.78 \pm 0.28)\%$ , respectively.

Similar to  $\Delta a_\mu^{\text{had,LO}}[\pi\pi, \tau]$ , we have evaluated the IB corrections to

$$\Delta\mathcal{B}_{\pi^-\pi^0}^{\text{CVC}} = \frac{3}{2} \frac{\mathcal{B}_e |V_{ud}|^2}{\pi\alpha^2 m_\tau^2} \int_{s_{\text{min}}}^{m_\tau^2} ds s \sigma_{\pi^+\pi^-}^0(s) \times \left(1 - \frac{s}{m_\tau^2}\right)^2 \left(1 + \frac{2s}{m_\tau^2}\right) \left[\frac{S_{\text{EW}}}{R_{\text{IB}}} - 1\right], \quad (9)$$

where  $s_{\text{min}} = (m_{\pi^-} + m_{\pi^0})^2$ . The results are summarised in Table IV. The corresponding  $\mathcal{B}_{\pi^-\pi^0}^{\text{CVC}}$  (Table V) is  $(24.78 \pm 0.17_{\text{exp}} \pm 0.22_{\text{IB}})\%$  and  $(24.92 \pm 0.21_{\text{exp}} \pm 0.22_{\text{IB}})\%$ , based on the combined  $e^+e^-$  data, including and excluding the KLOE data, respectively. The

<sup>5</sup> The use of the term standard deviation ( $\sigma$ ) in this context requires caution because the results discussed in this paper are mostly dominated by systematic uncertainties with questionable statistical properties.



TABLE V: Evaluated  $\mathcal{B}_{\pi^-\pi^0}^{\text{CVC}} (\times 10^{-2})$  from the  $e^+e^-$  data including and excluding KLOE data, respectively. The errors correspond to the experimental uncertainties with the statistical and systematical errors added in quadrature (but shown separately for individual experiments). The IB uncertainty of 0.22 is not explicitly quoted for the subcontributions.

Energy range (GeV)	Experiment	$\mathcal{B}_{\pi^-\pi^0}^{\text{CVC}} (\%)$	
		Incl. KLOE	Excl. KLOE
$m_{\pi^-} + m_{\pi^0} - 0.36$	Combined $e^+e^-$ (fit)	$0.03 \pm 0.00_{\text{exp}}$	
0.36 – 0.63	Combined $e^+e^-$	$1.96 \pm 0.03_{\text{exp}}$	$1.94 \pm 0.03_{\text{exp}}$
0.63 – 0.958	CMD2 03	$20.67 \pm 0.13_{\text{stat}} \pm 0.12_{\text{syst}}$	
	CMD2 06	$20.58 \pm 0.08_{\text{stat}} \pm 0.16_{\text{syst}}$	
	SND 06	$20.54 \pm 0.07_{\text{stat}} \pm 0.27_{\text{syst}}$	
	KLOE 08	$20.26 \pm 0.02_{\text{stat}} \pm 0.17_{\text{syst}}$	
	Combined $e^+e^-$	$20.40 \pm 0.14_{\text{exp}}$	$20.56 \pm 0.17_{\text{exp}}$
0.958 – $m_\tau$	Combined $e^+e^-$	$2.39 \pm 0.06_{\text{exp}}$	
Total	Combined $e^+e^-$	$24.78 \pm 0.17_{\text{exp}} \pm 0.22_{\text{IB}}$	$24.92 \pm 0.21_{\text{exp}} \pm 0.22_{\text{IB}}$

first error quoted corresponds to the experimental error and the second error due to uncertainties in the isospin-breaking corrections. It differs from the  $\tau$  measurement by  $(0.64 \pm 0.10_\tau \pm 0.28_{ee})\%$  and  $(0.50 \pm 0.10_\tau \pm 0.30_{ee})\%$ , respectively, which is still substantial, but less significant than the previous result [11, 13]. A graphical comparison between the IB-corrected  $\mathcal{B}_{\pi\pi^0}^{\text{CVC}}$  and the measured branching fractions  $\tau^- \rightarrow \pi^-\pi^0\nu_\tau$  [7–9, 14] is shown in Fig. 6. The  $\mathcal{B}_{\pi\pi^0}^{\text{CVC}}$  results are obtained using the  $e^+e^-$  data from CMD2, SND and KLOE in 0.63–0.958 GeV and the combined  $e^+e^-$  data in the other energy regions.

## VI. SUMMARY

We have revisited and updated the isospin-breaking corrections to  $\tau$  data in the  $2\pi$  mode, incorporating new ingredients in the long-distance radiative corrections and in the mass and width splittings of mesons that enter the pion form factors. We find that the  $\tau$  and  $e^+e^-$  spec-

tral functions from CMD-2 and SND are now marginally consistent, while a disagreement with the KLOE measurement remains. The corrected  $\tau$ -based result for the Standard Model prediction of the muon  $g-2$  is now 1.9 standard deviations lower than the direct measurement, coming closer to the  $e^+e^-$  value. Similarly, the prediction of the  $\tau^- \rightarrow \pi^-\pi^0\nu_\tau$  branching fraction with  $e^+e^-$  annihilation data exhibits a reduced discrepancy with the  $\tau$  measurement.

We are indebted to H. Hayashii for providing the correlation of the  $\tau$  mass spectrum of the Belle data. We thank R. Barbieri, C. Bouchiat, G.V. Fedotov, E.A. Kuraev, W. Marciano and A. Vainshtein for helpful discussions. GLC and GTS acknowledges Conacyt (Mexico) for financial support. This work is supported by National Natural Science Foundation of China (10491303, 10825524, 10775142), 100 Talents Program of CAS (U-25) and the Talent Team Program of CAS (KJCX2-YW-N45).

- |   |  |
|---|--|
| <p>[1] CMD-2 Collaboration (R.R. Akhmetshin <i>et al.</i>), Phys. Lett. B 578, 285 (2004) [arXiv:hep-ex/0308008];</p> <p>[2] CMD-2 Collaboration (V. M. Aulchenko <i>et al.</i>), JETP Lett. 82, 743 (2005) [arXiv:hep-ex/0603021]; CMD-2 Collaboration (R. R. Akhmetshin <i>et al.</i>), JETP Lett. 84, 413 (2006) [arXiv:hep-ex/0610016]; CMD-2 Collaboration (R.R. Akhmetshin <i>et al.</i>), Phys. Lett. B 648, 28 (2007) [arXiv:hep-ex/0610021].</p> <p>[3] SND Collaboration (M. N. Achasov <i>et al.</i>), JETP Lett. 103, 380 (2006) [arXiv:hep-ex/0605013].</p> <p>[4] KLOE Collaboration (F. Ambrosino <i>et al.</i>), Phys. Lett. B 670 285 (2009) [arXiv:0809.3950 (hep-ex)].</p> <p>[5] R. Alemany, M. Davier and A. Hoecker, Eur. Phys. J. C 2, 123 (1998).</p> | <p>[6] ALEPH Collaboration (R. Barate <i>et al.</i>), Z. Phys. C76, 15 (1997).</p> <p>[7] ALEPH Collaboration (S. Schael <i>et al.</i>), Phys. Rep. 421, 191 (2005).</p> <p>[8] CLEO Collaboration (S. Anderson <i>et al.</i>), Phys. Rev. D 61, 112002 (2000).</p> <p>[9] OPAL Collaboration (K. Ackerstaff <i>et al.</i>), Eur. Phys. J. C 7, 571 (1999).</p> <p>[10] M. Davier, S. Eidelman, A. Hoecker and Z. Zhang, Eur. Phys. J. C 27, 497 (2003).</p> <p>[11] M. Davier, S. Eidelman, A. Hoecker and Z. Zhang, Eur. Phys. J. C 31, 503 (2003).</p> <p>[12] G.W. Bennett <i>et al.</i>, Phys. Rev. Lett. 89, 101804 (2002).</p> <p>[13] M. Davier, Nucl. Phys. Proc. Suppl. 169, 288 (2007).</p> |
|---|--|

- [14] Belle Collaboration (M. Fujikawa *et al.*), Phys. Rev. D 78, 072006 (2008).
- [15] The HVPTools source code (C++, relying on ROOT functionality) and database (XML format) can be made publicly available. Please contact the authors.
- [16] H. Hayashii, private communication.
- [17] L3 Collaboration (M. Acciarri *et al.*), Phys. Lett. B 345, 93 (1995).
- [18] DELPHI Collaboration (J. Abdallah *et al.*), Eur. Phys. J. C 46, 1 (2006).
- [19] Particle Data Group (C. Amsler *et al.*), Phys. Lett. B 667, 1 (2008).
- [20] Y.S. Tsai, Phys. Rev. D 4, 2821 (1971) [Erratum-ibid. D 13, 771 (1976)].
- [21] H.B. Thacker and J.J. Sakurai, Phys. Lett. 36, 103 (1971).
- [22] CKMfitter Group (J. Charles *et al.*), Eur. Phys. J. C 41, 1 (2005); updates from <http://ckmfitter.in2p3.fr>.
- [23] M. Davier, A. Hoecker and Z. Zhang, Rev. Mod. Phys. 78, 1043 (2006).
- [24] A. Sirlin, Rev. Mod. Phys. 50, 573 (1978) [Erratum-ibid. 50, 905 (1978)]; W. Marciano and A. Sirlin, Phys. Rev. Lett. 61, 1815 (1988); A. Sirlin, Nucl. Phys. B 196, 83 (1982).
- [25] E. Braaten and C.S. Li, Phys. Rev. D 42, 3888 (1990).
- [26] J. Erler, Rev. Mex. Fis. 50, 200 (2004).
- [27] J.S. Schwinger, “Particles, Sources and Fields”, Vol. 3, Reading, Massachusetts (1989); see also, M. Drees and K. Hikasa, Phys. Lett. B 252, 127 (1990)
- [28] V. Cirigliano, G. Ecker and H. Neufeld, Phys. Lett. B 513, 361 (2001); JHEP 0208, 002 (2002).
- [29] For a recent review, see *e.g.* J. Portoles, Nucl. Phys. Proc. Suppl. 169,3 (2007).
- [30] J. Wess and B. Zumino, Phys. Lett. B 37, 95 (1971); E. Witten, Nucl. Phys. B 223, 422 (1983).
- [31] A. Flores-Tlalpa F. Flores-Baez, G. Lopez Castro and G. Toledo Sanchez, Phys. Rev. D 74, 071301 (2006); Nucl. Phys. Proc. Suppl. 169, 250 (2007).
- [32] T. Kinoshita and A. Sirlin, Phys. Rev. 113, 1652 (1959).
- [33] G.J. Gounaris and J.J. Sakurai, Phys. Rev. Lett. 21, 244 (1968).
- [34] J.H. Kühn and A. Santamaria, Z. Phys. C 48 (1990) 445.
- [35] K. Maltman and C.E. Wolfe, Phys. Rev. D 73, 013004 (2006).
- [36] M. Benayoun *et al.*, Eur. Phys. J. C 55, 199 (2008).
- [37] F. Guerrero and A. Pich, Phys. Lett. B 412, 382 (1997).
- [38] F. Flores-Baez, G. Lopez Castro and G. Toledo Sanchez, Phys. Rev. D 76, 096010 (2007).
- [39] See *e.g.* J.J. Sakurai, “Currents and Mesons”, The university of Chicago press, 1969.
- [40] KLOE Collaboration (A. Aloisio *et al.*), Phys. Lett. B 561, 55 (2003).
- [41] S.J. Brodsky and E. de Rafael, Phys. Rev. 168, 1620 (1968).
- [42] F. Flores-Baez and G. López Castro, Phys. Rev. D 78, 077301 (2008).
- [43] S. Dubinsky, A. Korchin, N. Merenkov, G. Pancheri and O. Shekhovtsova, Eur. Phys. J. C 40, 41 (2005) [arXiv:hep-ph/0411113]
- [44] NA7 Collaboration (S.R. Amendolia *et al.*), Nucl. Phys. B 277, 168 (1986).
- [45] J. Prades, E. de Rafael and A. Vainshtein, arXiv:0901.0306 (hep-ph).
- [46] Muon  $g - 2$  Collaboration (G.W. Bennett *et al.*), Phys. Rev. D 73, 072003 (2006).
- [47] A. Hoecker and W. Marciano, “The Muon Anomalous Magnetic Moment” in [19]; update for 2009 in preparation (to appear at <http://pdglive.lbl.gov>).
- [48] K. Hagiwara, A.D. Martin, D. Nomura and T. Teubner, Phys. Lett. B 649, 173 (2007).
- [49] F. Jegerlehner, Acta Phys. Polon. B 38, 3021 (2007) [arXiv:hep-ph/0703125]; Nucl. Phys. Proc. Suppl. 181-182, 26 (2008).